Isotropic convection scenarios in an anisotropic fluid

Á.Buka[2], B.Dressel[1], L.Kramer[1] and W.Pesch[1],
[1] *Physikalisches Institut, Universität Bayreuth, D-95440 Bayreuth, Germany*
[2] *Research Institute for Solid State Physics and Optics, Hungarian Academy of Sciences, H-1525 Budapest, P.O. Box 49, Hungary*
(Dated: May 19, 2004)

We study a new variant of electroconvection using a homeotropically aligned nematic liquid crystal. The novelty of this system is a direct transition to roll- or square-type patterns controlled by the frequency of the applied voltage with a rich crossover scenario and strong influence of the ZigZag instability even at onset. From the weakly nonlinear theory and simulations of an adapted Swift-Hohenberg model one can understand essential features of the phase diagram. In particular we find a quasiperiodic pattern with square symmetry.

PACS numbers: PACS numbers: 47.54.+r, 47.20.Lz 61.30.Gd,

Nonequilibrium transitions in spatially extended continuum systems lead to a wide variety of fascinating patterns. The basic elements are stripes (or rolls), squares and (under some proviso) hexagons, which are the only simple *periodic* patterns that appear directly via a supercritical bifurcation in isotropic quasi-twodimensional systems [1]. In rare cases there is a direct (supercritical) transition to a *disordered state*. To our knowledge a direct transition to a long-wave modulated quasiperiodic pattern has never been described before.

The common framework for the description near threshold is given by universal amplitude equations, which are governed by the symmetries of the problem, while largely independent of physical details [2]. The underlying concepts have been mainly developed and tested in Rayleigh-Bénard convection (RBC) driven by a temperature gradient in a horizontal layer of a simple fluid [1, 3, 4]. The competition between the prevailing stripes (rolls) and hexagons near threshold is well understood [1]. Although squares are observed in quite diverse systems [5, 9] studies of their nonlinear aspects are scarce.

Here we study electroconvection (EC) near threshold in a homeotropically aligned nematic liquid crystal exhibiting a direct transition to EC, which represents a new model system for isotropic pattern formation. Unlike in other systems, here the competition between rolls and squares can be systematically investigated at small amplitude in the same cell with large-aspect ratio [10] by merely changing the frequency of the applied voltage. Since the system is driven by an ac voltage there is an intrinsic reflection symmetry about the mid plane. Thus the quadratic resonance coupling leading to competing hexagons is absent.

The patterns in the experiment and in large-aspect ratio simulations near threshold exhibit modulations with a slow dynamics. The global orientation of the patterns is random. The modulations are of ZigZag (ZZ) type in the roll regime (see Fig. 1) and undulated in the regime of squares ("soft squares", see Fig. 2). The ZZ modulations are always manifestly disordered. The undulations of the soft squares are initially irregular (see [11], Fig. 3). In the experiments they become after long time nearly periodic in space (see Fig. 2a) with a very slow persistent dynamics, in agreement with most simulations. The simulations are based on a suitably chosen Swift-Hohenberg equation (SHE), which is a standard approach in isotropic pattern formation.

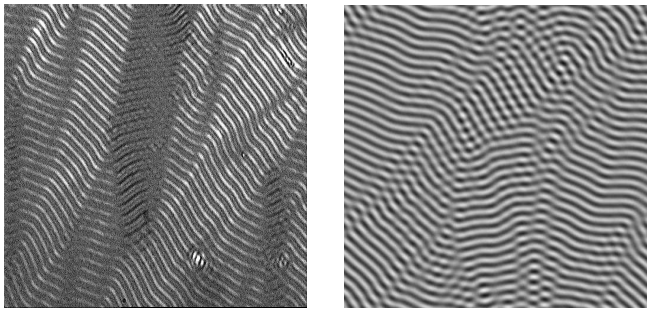

FIG. 1: Snapshots of ZZ roll patterns in experiment (a) ($\epsilon = 0.038$, $\omega/\omega^*_{exp} = 0.18$) and in simulation (b) of the SH-equation ($\epsilon = 0.006$, $\omega/\omega^*_{theo} = 0.16$). Definitions are given later in the text.

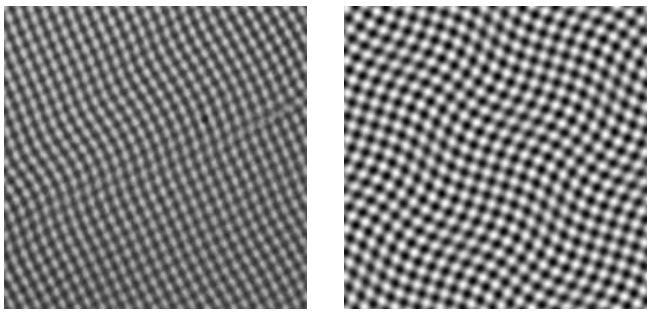

FIG. 2: Snapshots of "soft" square patterns slightly above ω^* (a) experiment ($\epsilon = 0.038$, $\omega/\omega*_{exp} = 1.16$) and (b) simulations of the SH-equation ($\epsilon = 0.022$, $\omega/\omega^*_{theo} = 1.07$).

Interestingly, for some parameters, and then for large classes of initial conditions, all defects are pushed out in

the simulations and the undulations become completely regular, i.e. the soft squares settle into a static, spatially quasiperiodic attractor (see Fig. 2b; the regular pattern at this ω was found for $\epsilon \leq 0.022$).

The scenario originates in particular from the well-known transverse modulational ZZ instability of rolls, which is present in squares as well, since it acts on each roll system individually (in contrast to resonant hexagons, where the ZZ instability is suppressed) [9]. It is driven largely by the mean flow, which here acts differently than in RBC and is crucial already at threshold.

Thus we have the unique case of a direct transition to a *stationary pattern* that is destabilized by long-wave instabilities leading either to disorder or to an ordered, quasiperiodic pattern. Other experimentally accessible direct transitions to long-wave destabilized patterns involve Hopf bifurcations to *travelling waves* [12, 13] or the presence of an additional Goldstone mode [14]. Alternatively, destabilisation of rolls at onset can be prompted by a short-wave instability, as in rotating RBC [15]. In all these cases the destabilization leads to disorder only.

Nematics are characterized by the mean orientation of their rod-like molecules along the director $\hat{\mathbf{n}}$ [16]. The anisotropy is reflected in the material parameters such as the conductivity tensor $\sigma_{ij} = \sigma_\perp \delta_{ij} + \sigma_a n_i n_j$, where $\sigma_a = \sigma_\parallel - \sigma_\perp$ and $\sigma_\parallel$, $\sigma_\perp$ are the conductivities parallel and perpendicular to $\hat{\mathbf{n}}$ and analogously the dielectric permittivity tensor ε_{ij}. Studying isotropic convection in these substances might look surprising since EC is a favorite model system for *anisotropic* convection. However, then the internal anisotropy of the material is expressed by external coupling as in the standard *planar* setup by anchoring the director along an axis parallel to the bounding plates [17]. In contrast, our experiments on isotropic EC employ *homeotropically* aligned cells, where the director is oriented perpendicular to the confining plates and thus parallel to the applied ac-voltage $U\cos(\omega t)$. We use a new nematic with $\sigma_a < 0$ and $\varepsilon_a = \varepsilon_\parallel - \varepsilon_\perp > 0$ which exhibits a direct transition to EC at a critical voltage U_c (for details see [18]). The frequency ω is kept below a cutoff frequency with $\omega_{cut}\tau_q \approx 0.7$ ("conduction regime"), where $\tau_q = \varepsilon_0\varepsilon_\perp/\sigma_\perp$ is the charge relaxation time.

The stability diagram of the rolls obtained from the linear and the nonlinear analysis of the full nematohydrodynamic equations (NHDE) is consistent with the experiments [18]. We find a direct transition to squares at threshold for frequencies above $\omega^*_{theo}\tau_q \approx 0.60$, which correlates well with the experimentally observed crossover to squares at $\omega^*_{exp}\tau_q \approx 0.55$ (for $\omega \geq \omega^*_{exp}$ the cell is filled only with squares at onset). In Fig. 3 we show the full stability diagram in the ϵ, q plane ($q = |\vec{q}|$) for a frequency slightly below ω^*_{theo}. Rolls with wavenumber q exist above the neutral curve N, which near threshold has the form $\epsilon_N(q) = \xi^2(q - q_c)^2$ where ξ is the coherence length. Outside the region limited by the line $R(q)$ the

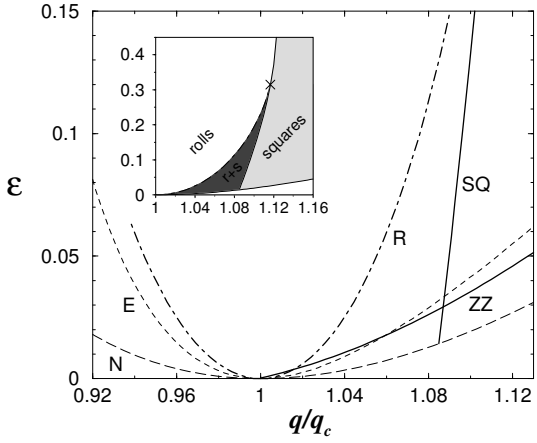

FIG. 3: Stability diagram of rolls with wavenumber q below the transition frequency to squares at $\omega/\omega^*_{theo} = 0.82$. Above the neutral curve (N, dashed) the Eckhaus (E, thin dashed) and ZZ instability (ZZ, thick solid) are shown. The line R shows the cross-roll instability. To the right of the SQ line there exist amplitude-stable squares. The inset shows the merging of the R with the SQ line (cross) at higher values of ϵ and the regions where one may expect rolls, rolls+squares (r+s), and squares.

rolls become unstable to growth of transverse rolls with wavenumbers q_{tr}. To the left of the line SQ, which meets the neutral curve at $(\epsilon_{SQ},\ q_{SQ})$, q is not contained in the band of q_{tr}. Then the perturbations do not saturate to stable rectangles, but initiate a wavelength-changing process of the roll system. To the right of the line SQ there exist destabilizing cross-roll processes with $q_{tr} = q$, which lead to amplitude-stable square patterns. When increasing ω the point (ϵ_{SQ}, q_{SQ}) moves down along the neutral curve, meets at ω^*_{theo} the threshold $(\epsilon = 0, q = q_c)$ and moves again upwards the neutral curve to the left for $\omega > \omega^*_{theo}$. Also, as ω reaches ω^*_{theo} the stable roll region inside the line $R(q)$ collapses to zero. For $\omega > \omega^*_{theo}$ a similar, parabolic stable region of squares opens up limited by the "rectangular instability" [9]. The ZZ line persists for squares, but at ω^*_{theo} its slope jumps to a higher value. This then describes fully the transition between the roll and square regimes.

Moreover, the ZZ line, which emerges linearily from the onset point $(\epsilon = 0,\ q = q_c)$, as is generic for isotropic systems, is tilted strongly to the right, see Fig. 3. Thus, already at onset the rolls become unstable against long-wavelength (transverse) ZZ modulations. This feature holds for all $\omega < \omega^*_{theo}$. By contrast, in RBC in simple fluids the ZZ line tilts to the left (except for large Prandtl number, where it is essentially vertical [1]). In both cases the tilt results mainly from mean-flow effects, which are generated by roll curvature. Whereas in EC the mean flow tends to reinforce the curvature, it acts stabilizing in RBC. The sign reversal in EC can be traced back to the influence of the Coulomb body force appearing in the

NHDE flow equation.

In the weakly nonlinear regime $0 \leq \epsilon = (U^2 - U_c^2)/U_c^2 < 0.1$ the stability diagram and salient features of the experimental patterns can be reproduced very well by the following generalized SHE model

$$\tau_0 \partial_t \psi = \left[\epsilon - \frac{\xi^2}{4q_c^2}(\Delta + q_c^2)^2 - \frac{e_3}{q_c^2}\epsilon(\Delta + q_c^2)\right]\psi - \left[\psi^3 + \frac{\gamma}{q_c^2}\psi(\nabla\psi)^2\right] + \frac{\beta}{q_c^4}\,\partial_i\left[(\partial_i\psi)(\partial_j\psi)^2\right] - \frac{1}{q_c^2}(\mathbf{U}\cdot\nabla)\psi, \quad (1)$$

$$(1 - c\Delta/q_c^2)\Delta\zeta = -\frac{g_1}{2q_c^2}(\nabla(\Delta\psi)\times\nabla\psi)\cdot\hat{\mathbf{z}} \quad (2)$$

with $\mathbf{U} = (\partial_y\zeta, -\partial_x\zeta)\,,\ c = 0.5$. Here $\psi(\mathbf{x}, t)$ portrays the pattern in the plane. Equations (1,2) are a generalization of the "simple SHE" where $e_3 = \gamma = \beta = g_1 = 0$. The linear term $\propto e_3$ describes a correction to the neutral curve which to cubic order in $q - q_c$ is given by $\epsilon_N = \xi^2(q - q_c)^2(1 + 2e_3(q - q_c))$ and the additional cubic nonlinearity $\sim \beta$ was introduced by [19] to capture bifurcations to squares. The term $\sim \gamma$ is well-known in the literature [2]. The description of the mean flow $\mathbf{U}$ is also well established [20]. Since the $\mathbf{U}$ derives from a Poisson equation it is of long range and acts without retardation. The term $\propto c$ is introduced to filter out short-scale contributions to $\mathbf{U}$ [21].

The coefficients of the SHE were related to the material parameters and to the frequency ω by mapping the stability diagram of the NHDE onto that of the SHE. The critical wavenumber q_c, the correlation time τ_0 and the correlation length ξ are known from the linear analysis [18]. With the Ansatz $\psi = Ae^{iq_c x} + Be^{iq_c y} + c.c.$ Eqs. (1,2) can be reduced to coupled amplitude equations for A, B. In the A-equation we arrive at the cubic nonlinearity $(-\mu|A^2|A - \nu|A^2|B)$ with $\mu = 3 + 3\beta + \gamma$ and $\nu = 2(3 + 2\beta + 2\gamma)$. The corresponding stability analysis in the NHDE shows that the cross coefficient ν/μ varies from 2.5 at $\omega = 0.1$ to 0.9 at $\omega = 0.7$ (it passes through 1 at ω^*_{theo}). This range can be covered in the SHE by varying continuously the coefficients β and γ. We fixed the ratio γ/β by the requirement that the SHE should reproduce the values for q_{SQ}, ϵ_{SQ} of the NHDE. Similarly, the strength g_1 of the mean flow coupling is fixed by equating the slope of the ZZ line $\epsilon_{ZZ}(q)$ at $\epsilon = 0$ from the NHDE (see Fig. 3) to that of the SHE which is given by $\epsilon_{ZZ}(q) = \xi^2(q - q_c)q_c/(G + e_3)$ with $G = (g_1 - 3\beta)/\mu$ for rolls (for squares one has $G = (g_1 - 9\beta)/(\mu + \nu)$). The contribution in G due to g_1 is about ten times larger than those due to β and e_3. Note that in the simple SHE the ZZ line is vertical and that g_1 is negative in RBC. For a parameterization of g_1, β, γ for $\omega \leq 0.7$, see [22].

Equations (1,2) have been solved by a standard pseudo-spectral code typically on a 256×256 grid with periodic boundary conditions on a domain which covers $25\lambda_c$ with $\lambda_c = 2\pi/q_c$. The relevant time scale is set by the horizontal diffusion time $t_H = 25^2\tau_0$. Starting with random initial conditions we let the system evolve at least for $5t_H$ which was sufficient to reach the steady states described below.

A representative simulation of the SHE immediately above threshold for ω well below ω^*_{theo} (ν/μ well above 1) yields the ZZ roll pattern shown in Fig. 1b. The patches in the corresponding experiment (Fig. 1a) show a variation in brightness since the underlying director field, not contained in the SHE, influences the optics. The structure is reminiscent of patterns found in the simple SHE at comparable ϵ only as transients when starting a simulation from a ZZ unstable roll pattern ($q < q_c$) or significantly above threshold as frozen states. There the q band has widened and certain resonance processes involving modes with $q < q_c$ become active [23]. In our case there is persistent slow dynamics. In RBC sharp structures in the roll pattern are smoothed out by mean flow, whereas in our system grain boundaries remain sharp despite the strong mean flow. We note that in Fig. 1 the value of ϵ is smaller in the simulation than in the experiment. The larger ϵ was needed to obtain sufficient contrast, but the pattern remains essentially the same in the experiments at the lower ϵ.

With increasing ω (still $\omega < \omega^*$) at small ϵ one observes in the simulations and in experiment an increase in the fraction of regions with crossed rolls, which gives the impression of a mixed state of rolls and squares. Increasing ϵ in the experiments (at $\omega < \omega^*_{exp}$) one finds a discontinuous transition to a state of perfect ("hard") squares with sharp boundaries between differently oriented domains [18]. In the simulations, upon increase of ϵ above ϵ_{cr}, the system tends to settle in a state of almost perfect, slightly undulated stationary squares with a somewhat larger wavenumber ($q > q_{SQ}$).

We have checked that by reducing g_1 in Eq. (2) this crossover to squares is suppressed. Thus, interestingly, the mean flow, which destabilizes the roll pattern, generates a selection process towards squares, which, if perfectly ordered, do not excite mean flow.

For $\omega > \omega^*_{theo}$ the simulations at small ϵ give soft squares except in the immediate vicinity of the threshold, where the long-wave ZZ instability is suppressed by finite-size effects and we find perfect squares. This is consistent with experiments (Fig. 2a) where one does not expect finite-size effects due to the large aspect ratio. We mention that no difference of the wavenumbers in the two directions (no rectangularity) could be observed within the experimental error of about 5%. In some simulations (for a class of parameters and initial conditions) the soft squares ended up in a pattern with perfectly periodic undulations, see Fig. 2b. This represents a quasiperiodic solution of Eqs.(1,2) with an exact cubic symmetry, i.e. invariance under rotation by $\pi/2$. Stationary solutions of this type are indeed expected to exist quite generally. Since the modulations are of long wavelength, an approximate description is given by the nonlinear phase equa-

tion for the rectangular instability proposed in [9] with equal modulation wavenumbers in the x and y direction. Quasiperiodic solutions are usually expected to be unstable, representing saddle points which separate stable periodic solutions with different wavevectors. When the periodic solutions themselves are destabilized, as is the case here, the quasiperiodic solutions may become stable. An analogous situation arises in roll patterns undergoing the ZZ instability. In anisotropic systems one then has stable undulated roll structures in the ZZ unstable regime [24]. Similar effects have been predicted for isotropic convection [25]. For $\epsilon \to 0$ the allowed modulation wavenumbers should tend to zero.

The transition to hard squares in our experiments with increasing ϵ (for $\omega > \omega^*_{exp}$ already at a fairly small $\epsilon \sim 0.1$) are not captured appropriately by the SHE model. We suggest that the hard squares represent a superlattice structure where several wavevectors interact to suppress the ZZ instability. Such superlattices, which often represent quasiperiodic structures, have been of considerable interest recently [26, 27]. They have been investigated experimentally in particular in the Faraday instability in cells with aspect ratio below about 50 [28].

In conclusion, we demonstrated that EC in homeotropic cells using a new nematic with $\sigma_a < 0$ and $\varepsilon_a > 0$ can give valuable insight into novel scenarios for isotropic pattern formation. A particularly intriguing feature is that mean flow, which in RBC is responsible for the skewed varicose instability and spiral defect chaos [29], here leads to a very mild form of disorder or even to the generation of an unconventional ordered pattern. In the future we plan to extract from weakly nonlinear theory a quantitative understanding of the soft square attractor, in particular its quasiperiodic manifestation. From simulations we hope to characterize better its occurance in parameter space and its regions of attraction. Also, a detailed description of the hard square pattern and the transition from soft to hard squares appears of interest. We expect similar phenomena in other systems provided the aspect ratio can be made comparably large. The ZZ instability may be replaced by some other long-wave destabilisation, e.g. the skewed-varicose instability.

We thank G. Pelzl for providing us with the substance. Financial support by OTKA-T031808 and EU network HPRN-CT-2002-00312 is gratefully acknowledged.

[1] F. H. Busse, Rep. Prog. Phys. **41**, 1929 (1978)
[2] M. C. Cross and P. C. Hohenberg, Rev. Mod. Phys. **65**, 851 (1993) and references therein.
[3] A. C. Newell, T. Passot and J. Lega, Annu. Rev. Fluid Mech. **25**, 709 (2000).
[4] E. Bodenschatz, W. Pesch und G. Ahlers, Annu. Rev. Fluid Mech. **32**, 709 (2000).
[5] Squares at onset are observed in RBC with poorly heat conducting boundaries, in agreement with the theory (see e.g. [6]). The recently observed square patterns in Bénard-Marangoni convection at onset [7] are at variance with the theoretical prediction of subcritical hexagons at threshold [8]. For other experimental systems see [9].
[6] P. Le Gal and V. Croquette, Phys. Fluids **31**, 3440 (1988); M. Westerburg and F. Busse, J. Fluid Mech., **432**, 351 (2001).
[7] W. A. Tokaruk, T.C.A. Molteno and S. W. Morris Phys. Rev. Lett., **84**, 3590 (2001).
[8] A. Engel and J. B. Swift, Phys. Rev. E **62**, 6540 (2001).
[9] R. B. Hoyle, in *Time-Dependent Nonlinear Convection*, P. A. Tyvand, ed., Computational Mechanics Publications, Southampton, 1998, p.51; Physica **D 67**, 198 (1993).
[10] The thickness of the nematic layer was $11\mu m$, its lateral extension $\sim 2 \times 2cm^2$. The wavelength of squares was $\sim 3\mu m$, so we had several thousand periods along any lateral direction.
[11] Á.Buka, B. Dressel, L.Kramer, and W.Pesch, Chaos (in press)
[12] P. Kolodner, S. Slimani, N. Aubry, and R. Lima, Physica (Amsterdam) **85D**, 165 (1995).
[13] M. Dennin, M. Treiber, L. Kramer, G. Ahlers, and D. Cannell, Phys. Rev. Lett, **76**, 319 (1996).
[14] A. G. Rossberg, A. Hertrich, L. Kramer, and W. Pesch, Phys. Rev. Lett. **76**, 4729 (1996).
[15] Y. Hu, R. E. Ecke, and G. Ahlers, Phys. Rev. Lett. **74**, 5040 (1995).
[16] P. G. de Gennes and J. Prost, *The Physics of Liquid Crystals*. Clarendon Press, Oxford, 1993;
[17] L. Kramer and W.Pesch, in *Pattern Formation in Liquid Crystals*, A. Buka and L. Kramer, editors (Springer-Verlag, New York, 1996);
[18] Á.Buka, B. Dressel, W. Otowski, K. Camara, T. Toth-Katona, L.Kramer, J. Lindau, G. Pelzl, and W. Pesch, Phys. Rev. **E 66**, 051713/1-8 (2002).
[19] C.J. Chapmann and M.R.E. Proctor. JFM **101**, 759 (1980)
[20] P. Manneville, J. Physique **44**, 759 (1983).
[21] H. S. Greenside und W. M. Coughran, Phys. Rev. A **30**, 398 (1984).
[22] $\beta = -0.1318 + 3.048\omega^2 - 1.092\omega^4$, $\gamma = -1.516 - 1.154\omega^2 - 1.326\omega^4$, $g_1 = 36.3 + 51.32\omega^2 + 411.51\omega^4$.
[23] A. C. Newell, R. Passot, N. Ercolani and R. Indik, J. Phys. II France , 1 (1995).
[24] E. Bodenschatz, M. Kaiser, L. Kramer, W. Pesch, A. Weber und W. Zimmermann, in "New Trends in Nonlinear Dynamics and Pattern Formation Phenomena: The Geometry of Nonequilibrium", Eds. P. Coullet and P. Huerre, NATO ASI Series B 237, Plenum Press, 1990, p. 111.
[25] F. H. Busse and M. Auer, Phys. Rev. Lett. **72**, 3178 (1994).
[26] B. Dionne, M. Silber, and A. C. Skeldon, Nonlinearity **10**, 321 (1997).
[27] A.M. Rucklidge, Phil. Trans. R. Soc. Lond. bf A 361, 2649 (2003).
[28] H. Arbell and J. Fineberg, Phys.Rev. **E 65**, 036224 (2002).
[29] S. W. Morris, E. Bodenschatz, D. S. Cannell und G. Ahlers, Phys. Rev. Lett. **71**, 2026 (1993).